

# Interface Chemistry of Nanostructured Materials: Ion Adsorption on Mesoporous Alumina

Yifeng Wang,<sup>\*,†,1</sup> Charles Bryan,<sup>\*</sup> Huifang Xu,<sup>†</sup> Phil Pohl,<sup>‡</sup> Yi Yang,<sup>§</sup> and C. Jeffrey Brinker<sup>†,§</sup>

<sup>\*</sup>Sandia National Laboratories, Carlsbad, New Mexico 88220; <sup>†</sup>Department of Earth and Planetary Sciences, University of New Mexico, Albuquerque, New Mexico 87131-1116; <sup>‡</sup>Sandia National Laboratories, Albuquerque, New Mexico 87185; and <sup>§</sup>Advanced Materials Laboratory, University of New Mexico, Albuquerque, New Mexico 87106

Received January 7, 2002; accepted June 28, 2002; published online September 16, 2002

This paper presents a part of our work on understanding the effect of nanoscale pore space confinement on ion sorption by mesoporous materials. Acid–base titration experiments were performed on both mesoporous alumina and alumina particles under various ionic strengths. The point of zero charge (PZC) for mesoporous alumina was measured to be  $\sim 9.1$ , similar to that for nonmesoporous alumina materials, indicating that nanoscale pore space confinement does not have a significant effect on the PZC of pore surfaces. However, for a given pH deviation from the PZC,  $(\text{pH} - \text{PZC})$ , the surface charge per mass on mesoporous alumina was as much as 45 times higher than that on alumina particles. This difference cannot be fully explained by the surface area difference between the two materials. Our titration data have demonstrated that nanoscale confinement has a significant effect, most likely via the overlap of the electric double layer (EDL), on ion sorption onto mesopore surfaces. This effect cannot be adequately modeled by existing surface complexation models, which were developed mostly for an unconfined solid–water interface. Our titration data have also indicated that the rate of ion uptake by mesoporous alumina is relatively slow, probably due to diffusion into mesopores, and complete equilibration for sorption could take 4–5 min. A molecular simulation using a density functional theory was performed to calculate ion adsorption coefficients as a function of pore size. The calculation has shown that as pore size is reduced to nanoscales ( $< 10$  nm), the adsorption coefficients of ions can vary by more than two orders of magnitude relative to those for unconfined interfaces. The prediction is supported by our experimental data on Zn sorption onto mesoporous alumina. Owing to their unique surface chemistry, mesoporous materials can potentially be used as effective ion adsorbents for separation processes and environmental cleanup. © 2002 Elsevier Science (USA)

**Key Words:** nanostructured materials; mesoporous alumina; electric double layer; ion sorption; density functional theory.

## INTRODUCTION

Functional materials that can effectively remove specific ions from aqueous solutions are of great interest for chemical separation and environmental cleanup applications. Recent progress in

the synthesis of nanostructured materials opens a new arena for developing such materials. Mesoporous materials synthesized using supramolecular templating processes (1–6) have attracted particular attention, due to their large specific surface area and controllable nanoscale pore size and geometry. Mesoporous silica with a monolayer of thiol (-SH) groups grafted on its pore surface displays a high sorption capacity for removing mercury from aqueous solutions (7, 8). Uncalcined mesoporous silicate materials synthesized with hexadecyltrimethylammonium bromide as a template are able to remove significant amounts of trichloroethylene and tetrachloroethylene from water (9), while calcined mesoporous silicates or titanosilicates were found to have the capability to remove copper, lead, and uranyl ions from aqueous solutions (10–12). Furthermore, an ordered mesoporous anion-exchange inorganic/organic hybrid resin has been suggested for radionuclide separation (13).

Various mesoporous materials have been synthesized using self-assembled supramolecular templating processes (1–6). Self-assembly is the spontaneous organization of materials through noncovalent interactions. It typically employs molecules of low symmetry that are programmed to organize into well-defined supramolecular assemblies. Most common are amphiphilic surfactant molecules or polymers composed of hydrophobic and hydrophilic parts. Above a critical concentration, surfactants in aqueous solution assemble into micelles, spherical or cylindrical structures that keep the hydrophilic parts of the surfactant in contact with water while shielding the hydrophobic parts within the micellar interior. Further increases in surfactant concentration result in the self-organization of micelles into periodic hexagonal, cubic, or lamellar mesophases. Inorganic precursors then precipitate on the surfactant structural templates. Inorganic mesoporous materials are obtained through removal of surfactants by chemical methods or calcination. Materials synthesized as such would have controllable nanoscale pore size and pore geometry and therefore provide an ideal system for studying the effect of nanoscale confinement on ion sorption.

The detailed mechanism of ion sorption by mesoporous materials is yet to be understood. It is generally known that a condensed phase could exhibit different physical and chemical properties than its bulk phase as its dimension was reduced

<sup>1</sup> To whom correspondence should be addressed. Fax: (505) 234-0061. E-mail: ywang@sandia.gov.

to a nanometer scale (14, 15). For a given mesoporous material, two factors are expected to control the ion sorption capability of the material: the accessible pore surface area and the effect of nanoscale pore space confinement. The former is determined by the geometry and connectivity of mesopores and, to some degree, can be optimized by controlling the formation of an appropriate mesophase during material synthesis (5, 6). A uniform pore structure with well-defined channels has been shown to have a great advantage over a disordered pore network in terms of the access of guest species to the binding sites (16). One direct consequence of nanoscale pore space confinement is the overlap of the electric double layer (EDL) within a mesopore, creating a surface complexation environment different from that for an unconfined surface. This overlap certainly affects overall ion sorption on mesoporous materials. In this paper, we present the results of our pH titration and ion sorption experiments with mesoporous alumina and of the related molecular simulations. We want to demonstrate the importance of nanoscale pore space confinement for ion uptake by mesoporous materials.

## EXPERIMENTAL SECTION

### Materials

Mesoporous alumina was obtained from Aldrich Chemical Company, Inc. The pore size of this material is reported to be 6.5 nm. Transmission electron microscopic (TEM) images show that this material has a “wormhole-like” mesostructure (Fig. 1A). Mesopores are irregular and have dimensions of  $\sim 2 \times 2 \times 10$  nm. The surface area of the mesoporous alumina was measured to be  $\sim 284$  m<sup>2</sup>/g, consistent with reported values (17). Lattice fringes in Fig. 1B indicate that the material is composed of amorphous alumina and nanocrystalline particles. These crystallites are identified to be  $\gamma$ -Al<sub>2</sub>O<sub>3</sub> from electron diffraction patterns. For a comparison between mesoporous and nonmesoporous materials, 80–200 mesh activated alumina particles were purchased from Fisher Chemicals. Our TEM observation indicates that the outer rims of particles consist of an amorphous Al<sub>2</sub>O<sub>3</sub> phase and very closely resemble mesoporous alumina in chemical composition and crystallinity. The surface area of the activated alumina particles is determined to be 118 m<sup>2</sup>/g; the large surface area of the material is probably due to the presence of microfractures on particle surfaces. The surface areas of both mesoporous alumina and activated alumina particles were determined using a Micromeritics Gemini 2360 surface analyzer.

### Titration

pH titration experiments were conducted for both mesoporous alumina and 80–200 mesh alumina particles using a Mettler DL25 autotitrator. The titration was performed in three electrolyte solutions: deionized (D.I.) water, 0.01 M NaCl, and 0.1 M NaCl. For mesoporous alumina, 0.1 g of solid was added to 50 ml of electrolyte solution and then titrated with 0.0564 M NaOH. The titration time interval was set to 90 s (the maxi-

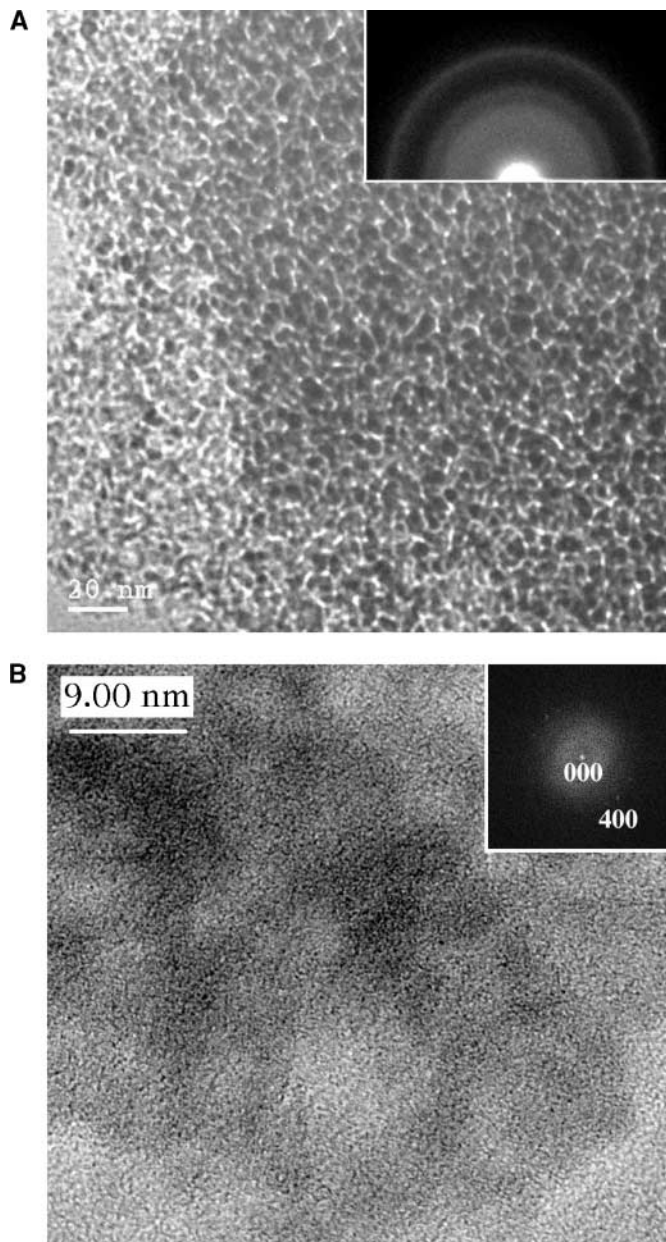


**FIG. 1.** Transmission electron microscopic (TEM) images of mesoporous alumina used in this study. (A) The material has a “worm hole-like” mesostructure. Mesopores are irregular and have dimensions of  $\sim 2 \times 2 \times 10$  nm. Inserted is a selected-area electron diffraction (SAED) pattern of the mesoporous alumina. (B) Lattice fringes indicate that the material is composed of nanoscale crystalline particles. From electron diffraction patterns, these crystallites are identified to be  $\gamma$ -Al<sub>2</sub>O<sub>3</sub>. Inserted is a fast Fourier transform (FFT) from an area of the HRTEM image showing a 2-Å spot corresponding to 400 reflection.

mum time allowed by the instrument) to minimize the possible effect of slow diffusion of ions in mesopores. For alumina particles, 1 g of solid was mixed with 50 ml of electrolyte solutions. The initial pH of the suspension was then adjusted to an acidic range by adding 2.3 ml of 0.0366 M HCl solution. The suspension was then titrated with 0.0564 M NaOH solution. As pH reequilibration between titration steps was extremely rapid,

the titration time interval was set to 20 s. All the titration experiments were performed under CO<sub>2</sub>-free conditions.

### Kinetic Studies

Either 0.1 g of mesoporous alumina or 1 g of 80–200 mesh alumina particles was mixed with 50 ml of deionized water and stirred for 5 min. A small amount of 0.094 M NaOH was then added to each suspension: 400  $\mu$ l for mesoporous alumina and 100  $\mu$ l for alumina particles. The pH of the suspension was then monitored at 10-s intervals using the autotitrator.

### pH/Sorption Edge Experiments

Each sample consisted of 20 ml of deionized water and 0.2 g of mesoporous alumina. The pH of each sample was adjusted using HCl or NaOH to obtain a range of pH values from 4 to 9, and then each suspension was spiked with Zn to produce an initial concentration of 10 ppm. The samples were then stirred continuously for 16–20 h, and the liquid was sampled, filtered with a 0.2- $\mu$ m syringe filter, and analyzed for Zn using an inductively coupled plasma optical emission spectrometer (ICP-OES).

## EXPERIMENTAL RESULTS

### Surface Charge

The titration results for both mesoporous alumina and alumina particles are shown in Fig. 2. The effect of ionic strength on pH titration curves follows a similar trend for both materials. All the titration curves cross over a common pH value, corresponding to a so-called point of zero charge (PZC), at which the surface charge becomes neutral and the effect of ionic strength on surface H<sup>+</sup> exchange diminishes. From Fig. 2, the PZC is estimated to be  $\sim$ 9.1 for mesoporous alumina and  $\sim$ 8.7 for alumina particles, both within the range reported for alumina oxides (18), thus indicating that the nanoscale pore space confinement does not have a significant effect on the PZC of pore surfaces. This observation is consistent with a general consideration that the PZC is an intrinsic property of a solid–water interface and is mainly determined by the chemical identity and crystallinity of the solid (18).

With the estimated PZC, the moles of surface charge per gram of material ( $Q$ ) can be calculated by (18)

$$Q = \frac{c_A - c_B + ([H^+] - [OH^-])V}{M} - Q_c \quad [1A]$$

$$Q_c = \left. \frac{c_A - c_B + ([H^+] - [OH^-])V}{M} \right|_{\text{pH}=\text{PZC}}, \quad [1B]$$

where  $c_A$  and  $c_B$  are moles of acid and base added;  $V$  is the volume ( $L$ ) of liquid;  $M$  is the mass of solid in the sample;  $Q_c$  is a correction term for the possible presence of additional acid or base in the initial materials; and  $[ ]$  indicates the concentrations of aqueous species. The concentrations of H<sup>+</sup> and OH<sup>-</sup> are calculated from the measured pH with a correction for ac-

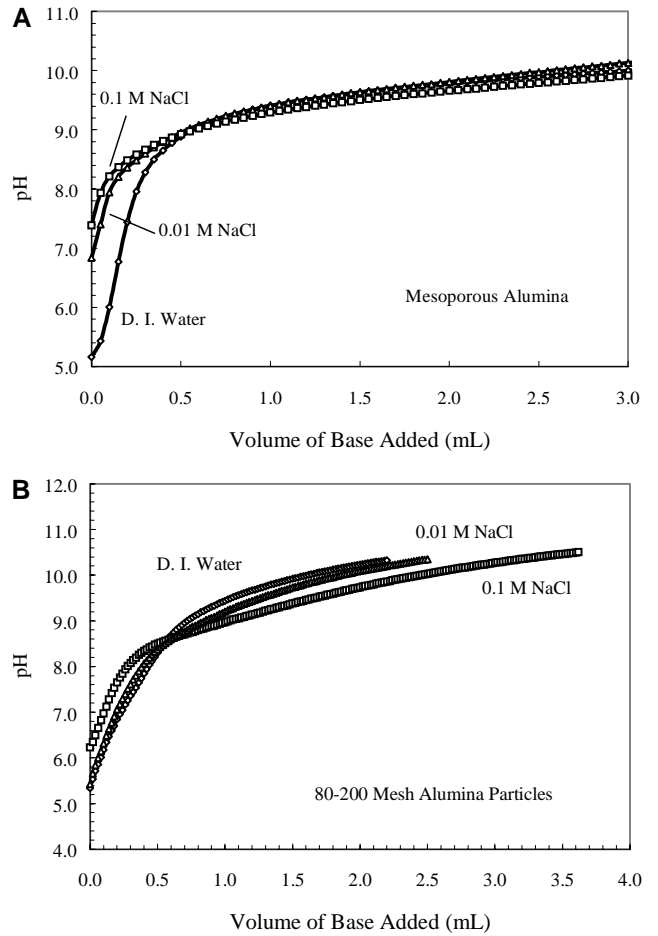


**FIG. 2.** Results of pH titration experiments. (A) 0.1 g mesoporous alumina in 50 ml electrolyte. (B) 1 g of 80–200 mesh alumina particles in 50 ml of solution. Each solid–liquid suspension was titrated with 0.0564 M NaOH in three electrolyte solutions: deionized (D.I.) water, 0.01 M NaCl, and 0.1 M NaCl. The point of zero charge (PZC) is defined as the pH at which all three titration curves cross.

tivity coefficients. For the mesoporous material, the correction term ( $Q_c$ ) is calculated to be negative, indicating the presence of additional acid in the initial material that needs to be taken into account in the surface charge balance calculation. This is confirmed by the observation that adding 0.1 g mesoporous alumina to 50 ml deionized water results in a pH of 5.0. The functional dependence of surface charge on solution ( $\text{pH} - \text{PZC}$ ) is shown in Fig. 3. The figure shows that, for a given ( $\text{pH} - \text{PZC}$ ), the surface charge per mass on mesoporous alumina can be as much as 45 times as high as that of the alumina particles, thus demonstrating the excellent ion sorption capability of mesoporous materials. Since the surface charges in mesoporous materials distribute within intraparticle nanoscale pores, in which differential movement between the solution and the pore surface is expected to be difficult, the measurement of these charges using an electrokinetic method might not be feasible.

For simplicity, the surface charge calculation in Eq. [1] ignores a possible contribution of dissolved aluminum species.

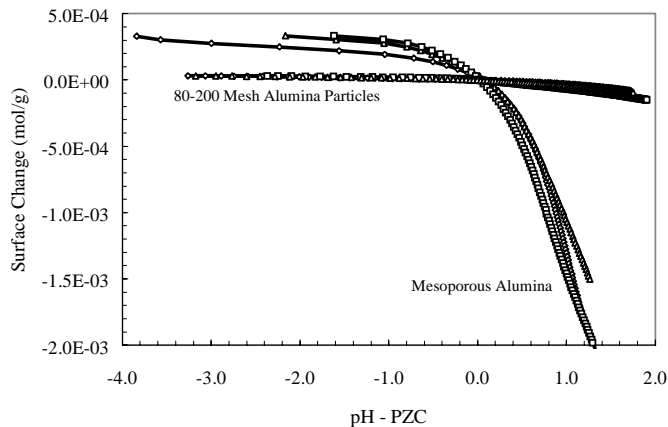


FIG. 3. Surface charge density as a function of (pH – PZC). For a given (pH – PZC), the surface charge per mass on mesoporous alumina can be as much as 45 times higher than that on alumina particles.

This approximation is reasonable because the total dissolved aluminum concentrations measured at the end of titration (i.e., at the high-pH end) are too low to account for the observed large surface charge difference (Table 1). Also, the large variations in the surface charge ratio between the two materials for different ionic strengths cannot be explained by the presence of dissolved aluminum species, because the effect of ionic strength on the activity coefficients of dissolved species are negligible under the relevant experimental conditions. To rule out the effect of a possible formation of a secondary surface layer on the surface charge calculation, a careful TEM observation was performed, which indicates that the surface structure and composition of both mesoporous and activated alumina particles remained intact and no surface layer was formed during the titration.

#### Acidity Constants

For pH values far from the PZC,  $Q \cong \{\text{SOH}_2^+\}$  for  $\text{pH} < \text{PZC}$  and  $Q \cong \{\text{SO}^-\}$  for  $\text{pH} > \text{PZC}$ , where  $Q$  is the surface charge

and  $\{\}$  indicates surface concentrations. Acidity constants of the materials used in the experiments can be calculated by

$$pK_1 = -\log\left(\frac{\{\text{SOH}\}[\text{H}^+]}{\{\text{SOH}_2^+\}}\right) \cong -\log\left(\frac{(S_{tot} - Q)[\text{H}^+]}{Q}\right) \quad [2A]$$

$$pK_2 = -\log\left(\frac{\{\text{SO}^-\}[\text{H}^+]}{\{\text{SOH}\}}\right) \cong -\log\left(\frac{Q[\text{H}^+]}{S_{tot} - Q}\right), \quad [2B]$$

where  $S_{tot}$  is the moles of total surface sites per gram of solid and is estimated to be 0.0023 mol/g for the mesoporous alumina and 0.00098 mol/g for the activated alumina particles, assuming 5 hydroxyls per  $\text{nm}^2$  (18). The calculated acidity constants for mesoporous alumina are shown in Fig. 4A. Linear extrapolation of  $pK$  to zero surface charge gives intrinsic acidity constants:  $pK_{1, \text{intr}} = 9.0$  and  $pK_{2, \text{intr}} = 10.3$ . For the approximations in Eq. [2] to be valid, the extrapolation uses only the data with pH values far from the PZC (Fig. 4A). It should be pointed out that the mesoporous material used in the experiments also includes a certain number of external (unconfined) surface sites. Here, however, we have no intention to differentiate these sites from the sites on mesopore surface, because the latter is dominant. The acidity constants obtained above mainly reflect the chemistry of mesopore surface. Similarly, the intrinsic acidity constants for activated alumina particles are estimated to be  $pK_{1, \text{intr}} = 7.7$  and  $pK_{2, \text{intr}} = 11.0$  (Fig. 4B). Using the relationship  $\text{PZC} = (pK_1 + pK_2)/2$ , we can estimate the PZC of 9.65 for mesoporous alumina and 9.35 for activated alumina particles. Both values, though slightly higher than those estimated directly from Fig. 2 (probably due to uncertainties associated with the linear extrapolation in Figs. 4A and B), are close to each other, again indicating little effect of nanoscale pore space confinement on the PZC of mesopore surfaces.

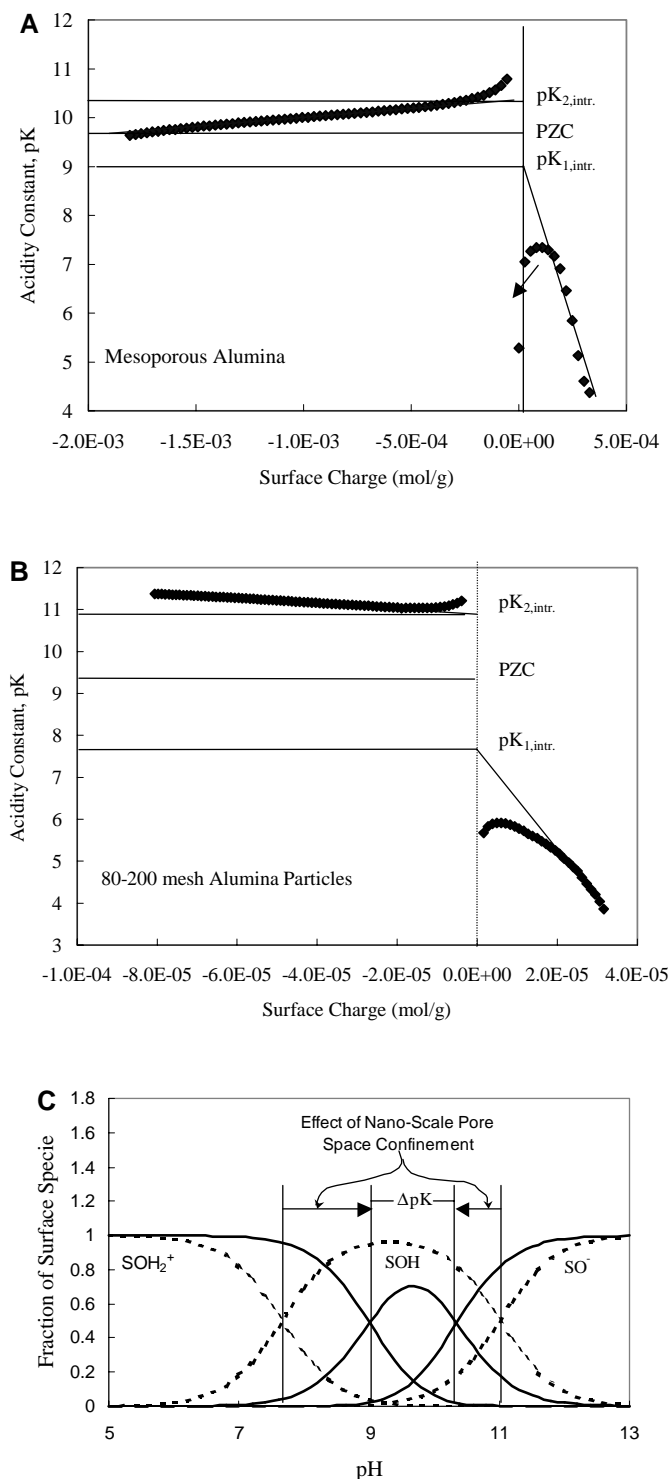
Interestingly enough, however, the pore space confinement does have a significant effect on the acidity constants of the materials. As shown in Fig. 4C, the separation between the two

TABLE 1  
Comparison of Dissolved Al Concentrations with Surface Charges Calculated Using Eq. [1]

	Dissolved Al (mol/l)		Surface charge (mol/l) <sup>a</sup>		Surface charge ratio, mesoporous alumina (mol/g)/alumina particles (mol/g) <sup>a</sup>	
	Alumina particles	Mesoporous alumina	Alumina particles	Mesoporous alumina	Not corrected for dissolved Al	Corrected for dissolved Al
D.I. water	0.00014	0.00079	0.0011	0.0026	24.1	19.3
0.01 M NaCl	0.00017	0.00065	0.0013	0.0021	15.9	12.7
0.1 M NaCl	0.00020	0.00073	0.0020	0.0029	14.8	12.3

Note. The dissolved Al concentrations were measured at the end of the titration experiments (at  $\text{pH} = 10$ ). For  $\text{pH} > 7$ ,  $\text{Al}(\text{OH})_4^-$  is a dominant species (30). The dissolution of alumina materials follows  $\text{AlO}_2/3 + 3/2\text{H}_2\text{O} = \text{Al}(\text{OH})_3 + \text{OH}^- = \text{Al}(\text{OH})_4^-$ ; i.e., one dissolved Al consumes one hydroxyl ion. For an easy comparison, both dissolved Al concentrations and surface charge densities are converted to the same unit (mol/l of solution). The calculated surface charge ratios, whether corrected for dissolved Al or not, are much larger than the surface area ratio between the two materials ( $=2.4$ ), indicating the effect of nanoscale pore space confinement. In each titration, either 0.1 g of mesoporous alumina or 1.0 g of alumina particles was added to a 50-ml solution.

<sup>a</sup> Negative charge.



**FIG. 4.** Acidity constants for mesoporous alumina (A) and activated alumina particles calculated (B) from the titration data in Fig. 3 using Eq. [2]. The calculation only includes the data points for the titration in D.I. water and far from the PZC. Linear extrapolation of  $pK$  to zero surface charge gives the intrinsic acidity constants  $pK_{1, \text{intr.}}$  and  $pK_{2, \text{intr.}}$ . (C) Surface speciation on mesoporous alumina (solid lines) and activated alumina particles (dashed lines). The separation between the two acidity constants,  $\Delta pK (= pK_2 - pK_1)$ , becomes significantly narrowed for the mesoporous alumina as compared to that for the alumina particles.

acidity constants,  $\Delta pK (= pK_2 - pK_1)$ , becomes significantly narrowed for the mesoporous alumina as compared to that for the alumina particles. As a result, within mesopores, neutral surface species SOH become depleted, and the pore surface tends to be either positively or negatively charged. This is one of the reasons that a mesoporous material has a much higher surface charge density than the corresponding nonmesoporous material. This result is consistent with the molecular modeling simulations presented below.

#### Effect of EDL Overlap

Two factors could contribute to the observed high surface charge density per mass of mesoporous materials: the large accessible pore surface area per mass and the effect of nanoscale pore space confinement. Since the surface area ratio of the mesoporous alumina to the activated alumina particles is only about 2.4 : 1, the surface area alone is not sufficient to account for the observed large surface charge difference between the two materials. In Fig. 5, the surface charges on the mesoporous material are plotted against those on the nonmesoporous material (alumina particles) for the corresponding (pH – PZC) values and ionic strengths. If the surface area were the only controlling factor, the resulting curves should fall on a single straight line with its slope defined by the ratio of the measured surface areas. As shown in Fig. 5, this is not the case, indicating that the nanoscale pore space confinement significantly contributes to surface charge development on mesoporous materials. For the systems we studied, this contribution is even more important than that from the surface area difference (Fig. 5). The effect of

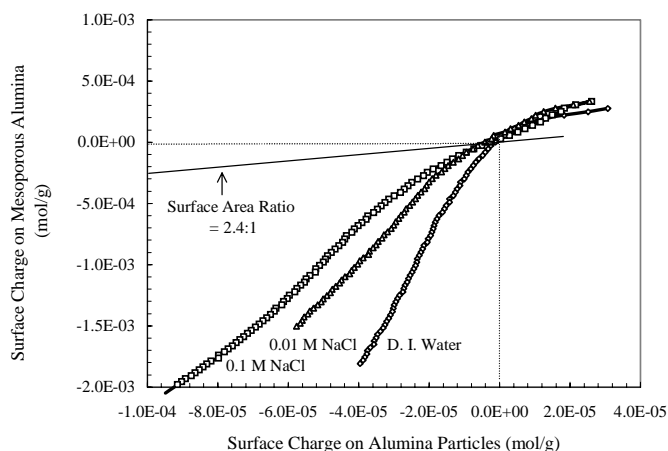


**FIG. 5.** Surface charge on mesoporous alumina vs surface charge on alumina particles for corresponding (pH – PZC) values and ionic strengths. For each ionic strength, the surface charges on both materials at various (pH – PZC) values are read from Fig. 3, and then the charges on one material are plotted against the charges on the other material for the same pH – PZC values. If the difference in surface charge between the two materials were controlled only by the surface area difference, the obtained surface charge vs surface charge curves would fall on a single straight line with its slope defined by the ratio of the measured surface areas ( $\approx 2.4 : 1$ ). The deviation from the straight line is attributed to the effect of nanoscale pore space confinement, probably via the overlap of the electric double layer.

the pore space confinement must arise from the change in the electric double layer structure (e.g., the overlap of EDL) within mesopores, because it strongly depends on ionic strength.

At a room temperature, the thickness of an electric double layer developed at a planar solid-water interface ( $L$ ) can be calculated as (18)

$$L = \frac{1}{3.29I^{1/2}} [\text{nm}], \quad [3]$$

where  $I$  is the ionic strength of the solution ( $M$ ). The thickness of EDL for ionic strengths of 0.01 and 0.1 M NaCl is estimated to be 1 and 3 nm respectively. As shown in Fig. 1A, the shortest dimension of the mesopores in mesoporous alumina is about 2 nm, and a significant overlap of EDL within the mesopores is thus expected.

Most existing surface complexation models have been developed for unconfined solid-water interfaces, for which the overlap of EDL is not a concern (18–20). The results shown in Fig. 5 demonstrate that such models are not adequate for predicting ion sorption onto mesoporous materials if the effect of nanoscale pore space confinement is not explicitly taken into account. Zhmud and his colleagues have attempted to develop a charge regulation model for the surface of porous matrices (21–23). In their model, a pore is represented by a cylindrical cavity, and the overlap of EDL is taken into account by diminishing the radius of the cylinder. Their model predicts a decrease in surface charge density with decreasing pore size. This prediction seems inconsistent with the titration data we obtained (Fig. 5). It should be pointed out that the terminology “electric double layer (EDL)” used in this paper only loosely refers to the electric charge distribution at mesopore surfaces, which does not necessarily resemble the EDL conceptualized for an unconfined interface. A generalization of the existing EDL concept to a nanoscale confined system is warranted.

#### Kinetics of Ion Sorption on Mesoporous Alumina

The ion uptake rates for both mesoporous alumina and alumina particles are shown in Fig. 6. Clearly, the rate for the meso-

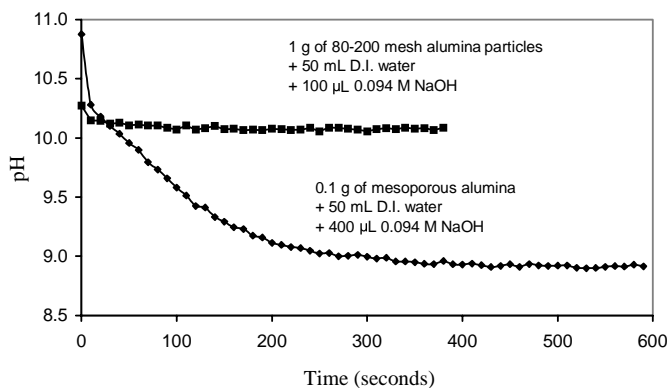


FIG. 6. Rates of ion uptake by mesoporous alumina and alumina particles. The rate for the mesoporous material is relatively slow, and it could take as long as 4–5 min for ion sorption to completely reach equilibrium.

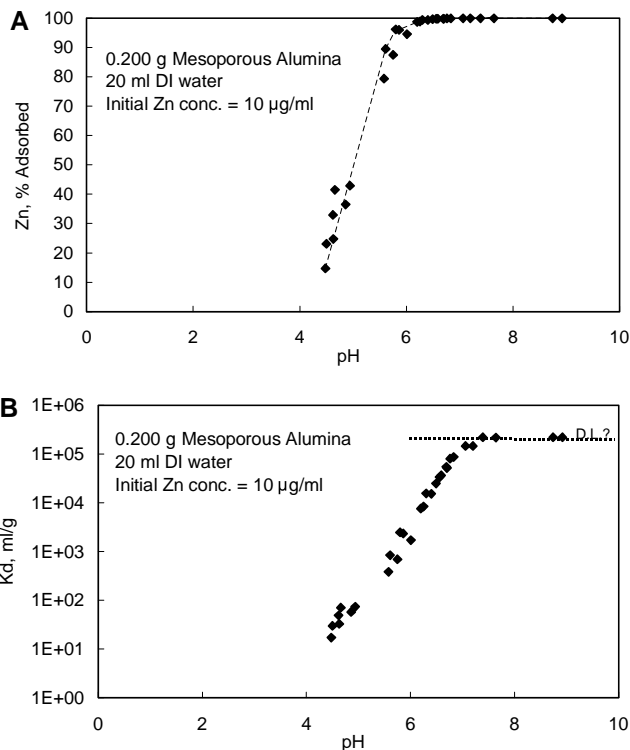


FIG. 7. Zn sorption on mesoporous alumina. The sorption edge is around the pH of 5. (A) percentage of Zn adsorbed vs pH; (B)  $K_d$  vs pH. The values shown above pH 7 are minimum values, based upon the detection limit for Zn.

porous material is relatively slow, and it could take as long as 4–5 min for ion sorption to completely reach equilibrium. The slow rate is due to ion diffusion in small pores. The surface area of mesoporous alumina might not be totally accessible during our titration experiments, because the maximum titration interval allowed by the instrument is 90 s. However, this kinetic effect is negligible in our surface charge balance calculations, because at a linear concentration scale, ion sorption can still reach more than 90% of completion over the 90-s time interval.

#### Zinc Sorption on Mesoporous Alumina

The pH/sorption edge for Zn sorption on mesoporous alumina is shown in Fig. 7. The sorption coefficient for mesoporous alumina is generally about two orders of magnitude higher than that reported for alumina particles (24), which seems consistent with the molecular modeling results summarized below. As a result, the sorption edge for a mesoporous material generally shifts to a lower pH and become sharper relative to that for a nonmesoporous material.

## MOLECULAR MODELING

To further clarify the effect of nanoscale pore space confinement, a molecular modeling simulation was performed for ion sorption between two parallel oxide surfaces. Modeling took place on two different scales of length. At the lowest level, a

quantum mechanical calculation was conducted to determine the size and charge distribution of adsorbates. The program DMol3 from MSI was used to carry out this geometry optimization modeling (25). The final simulations were performed using the density functional theory (DFT) described by Frink and Van Swol (26–28). In these simulations, the molecular detail is removed and only the component's density is determined based on the equilibrium of the system.

The DFT simulations were performed separately for two types of idealized oxide surfaces arranged in a parallel slit pore: a surface covered with hydroxyls and with a surface charge of 0.17 per hydroxyl, and a surface with all hydroxyls removed and with a surface charge of  $-0.54$  per oxygen atom. These values were determined using a charge equilibration method (29). The effect of pore space confinement was simulated by varying the separation between the two oxide surfaces while maintaining the same chemical potential for each chemical species as in the bulk solution. The sorption coefficient of an ion was then calculated as the ratio of the ion concentration integrated over the mesopore to the concentration in the bulk solution. Figure 8 shows the effect of pore size and surface chemistry on the adsorption coefficient. Note that the adsorption coefficients in the figure are normalized to the values corresponding to an unconfined system, i.e., to an infinite separation between the two parallel oxide surfaces in our modeling system, and therefore any deviation from 1 in these coefficients directly indicates the effect of nanoscale confinement on ion sorption. As expected, the surface charge has a significant effect on ion sorption. And more interestingly, this effect is greatly amplified as the pore space decreases to nanometer scales. This effect could become even more significant for ion sorption in a spherical or cylindrical confined environment. It is shown in Fig. 8 that for a divalent ion a mesoporous material with a pore size of 2 nm could have an adsorption coefficient two orders of magnitude higher or lower than the corresponding

nonmesoporous material. The typical scale for the confinement effect to become significant is less than 10 nm. The modeling results are generally consistent with the experimental data summarized above.

## CONCLUSIONS

Acid–base titration experiments were performed on both mesoporous alumina and alumina particles under various ionic strengths in order to clarify the control of mesopore structures on the surface chemistry of materials. The point of zero charge (PZC) for mesoporous alumina was measured to be 9.1, similar to that for nonmesoporous alumina particles, indicating that the nanoscale pore space confinement does not have a significant effect on the PZC of pore surfaces. However, for a given pH deviation from the PZC,  $(\text{pH} - \text{PZC})$ , the surface charge on mesoporous alumina was as much as 45 times higher than that on alumina particles. This difference cannot be fully explained by the surface area difference between the two materials. Our titration data have demonstrated that the nanoscale pore space confinement has a significant effect, most likely via the overlap of the electric double layer (EDL), on ion sorption on mesopore surface. This effect cannot be adequately modeled by the existing surface complexation models, which were developed mostly for unconfined solid–water interfaces. Our titration data have also indicated that the rate of ion uptake by mesoporous alumina is relatively slow, probably due to ion diffusion into mesopores, and complete equilibration for sorption could take 4–5 min. To further clarify the effect of nanoscale confinement on ion sorption, a molecular modeling calculation was performed using density functional theory. The calculation has shown that as the pore size is reduced to nanoscales ( $<10$  nm), the adsorption coefficients of ions can vary by more than two orders of magnitude relative to those on unconfined interfaces. The prediction is supported by our experimental data on Zn sorption on mesoporous alumina. Owing to their unique surface chemistry, mesoporous materials can potentially be used as effective ion adsorbents for separation processes and environmental cleanup.

## ACKNOWLEDGMENTS

Sandia is a multiprogram laboratory operated by Sandia Corporation, a Lockheed Martin company, for the United States Department of Energy (US DOE) under Contract DE-AC04-94AL8500. This research is supported by the DOE through a laboratory directed research and development (LRD) project and National Science Foundation (NER-021082). We thank Laurie Frink at Sandia National Laboratories for allowing us to use the TRAMONTO DFT code. We also thank A. T. Hubbard (the editor) and the anonymous reviewer for their insightful suggestions and comments.

## REFERENCES

1. Kresge, C. T., Leonowicz, M. E., Roth, W. J., Vartull, J. C., and Beck, J. S., *Nature* **359**, 710 (1992).
2. McCullen, S. B., Vartuli, J. C., Kresge, C. T., Roth, W. J., Beck, J. S., Schmitt, K. D., Leonowicz, M. E., Schlenker, J. L., Shih, S. S., and Lutner,

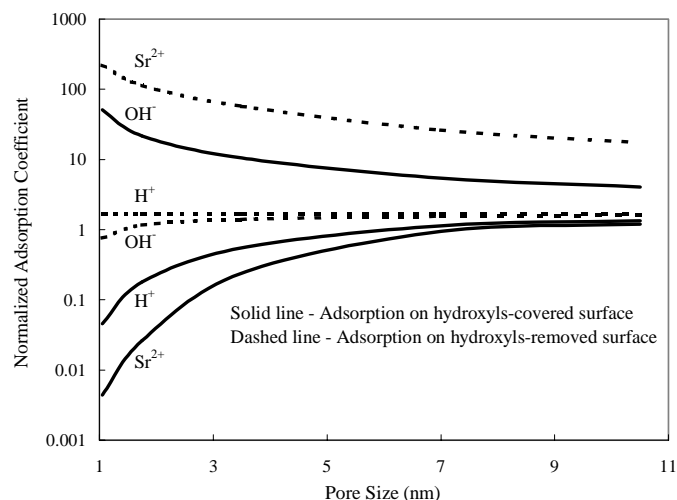


**FIG. 8.** Normalized adsorption coefficients calculated as a function of pore size. The adsorption coefficients are normalized to the values corresponding to an infinite separation between the two parallel oxide surfaces.

- J. D., in "Access in Nanoporous Materials" (T. J. Pinnavaia and M. F. Thorpe, Eds.), p. 1. Plenum, 1995.
3. Tanev, P. T., and Pinnavaia, T. J., in "Access in Nanoporous Materials" (T. J. Pinnavaia and M. F. Thorpe, Eds.), p. 13. Plenum, 1995.
  4. Anderson, M. T., Martin, J. E., Odinek, J., and Newcomer, P., in "Access in Nanoporous Materials" (T. J. Pinnavaia and M. F. Thorpe, Eds.), p. 29. Plenum, 1995.
  5. Brinker, C. J., Lu, Y., Sellinger, A., and Fan, H., *Adv. Mater.* **11**(7), 579 (1999).
  6. Selvam, P., Bhatia, S. K., and Sonwane, C. G., *Ind. Eng. Chem. Res.* **40**, 3237 (2001).
  7. Feng, X., Fryxell, G. E., Wang, L.-Q., Kim, A. Y., Liu, J., and Kemner, K. M., *Science* **276**, 923 (1997).
  8. Chen, X., Feng, X., Liu, J., Fryxell, G. E., and Gong, M., *Sep. Sci. Technol.* **34**, 1121 (1999).
  9. Zhao, H., Nagy, K. L., Waples, J. S., and Vance, G. F., *Environ. Sci. Technol.* **34**, 4822 (2000).
  10. Xu, Y.-M., Wang, R.-S., and Wu, F., *J. Colloid Interface Sci.* **209**, 380 (1999).
  11. Shin, Y. S., Burleigh, M. C., Dai, S., Barnes, C. E., and Xue, Z. L., *Radiochim. Acta* **84**, 37 (1999).
  12. Jung, J., Kim, J., Suh, J., Lee, J., and Ryu, S., *Water Res.* **35**, 937 (2001).
  13. Ju, Y. H., Webb, O. F., Dai, S., Lin, J. S., and Barnes, C. E., *Ind. Eng. Chem. Res.* **39**, 550 (2000).
  14. Adair, J. H., Li, T., Kido, T., Havey, K., Moon, J., Mecholsky, J., Morrone, A., Talham, D. R., Ludwig, M. H., and Wang, L., *Mater. Sci. Eng.* **R23**, 139 (1998).
  15. José-Yacamán, M., and Mehl, R. F., *Metall. Mater. Trans. A* **29**, 713 (1998).
  16. Mercier, L., and Pinnavaia, T. J., *Adv. Mater.* **9**, 500 (1997).
  17. Cabrera, S., Haskouri, J. E., Alamo, J., Beltrán, A., Beltrán, D., Mendioroz, S., Marcos, M. D., and Amorós, P., *Adv. Mater.* **11**, 379 (1999).
  18. Stumm, W., "Chemistry of the Solid–Water Interface." Wiley, New York, 1992.
  19. Davis, J. A., and Kent, D. B., in "Mineral–Water Interface Geochemistry" (M. F. Hochella, Jr. and A. F. White, Eds.), p. 177. Mineralogical Society of America, 1990.
  20. Dzombak, D. A., and Morel, F. M. M., "Surface Complexation Modeling: Hydrous Ferric Oxide." Wiley–Interscience, 1990.
  21. Zhmud, B. V., and Golub, A. A., *Colloids Surf. A* **105**, 173 (1995).
  22. Zhmud, B. V., *J. Colloid Interface Sci.* **183**, 111 (1996).
  23. Zhmud, B. V., Sonnefeld, J., and House, W. A., *J. Chem. Soc. Faraday Trans.* **93**, 3129 (1997).
  24. Tao, Z., Chu, T., Du, J., Dai, X., and Gu, Y., *Appl. Geochem.* **15**, 133 (2000).
  25. Molecular Simulations, Inc., "Cerius 2 User Guide." San Diego, 1997.
  26. Frink, L. J. D., and Van Swol, F., *J. Chem. Phys.* **106**(9), 3782 (1997).
  27. Frink, L. J. D., and Van Swol, F., *J. Chem. Phys.* **100**(12), 9106 (1994).
  28. Frink, L. J. D., and Van Swol, F., *J. Chem. Phys.* **108**(13), 5588 (1998).
  29. Rappe, A. K., and Goddard, W. A., *J. Phys. Chem.* **95**(8), 3358 (1991).
  30. Drever, J. I., "The Geochemistry of Natural Waters." Prentice–Hall, 1982.